Applicability of Modified Ritchie-Knott-Rice Failure Criterion to Predict the Occurrence of Cleavage Fracture under Residual Stress Field

Kenichi Ishihara[#1], Takeshi Hamada[#2], and Toshiyuki Meshii[*3]
[#] *Kobelco Research Institute, Inc.,*
1-5-5 Takatsukadai, Nishi-ku, Kobe, Hyogo, 651-2271, Japan
[*]*Faculty of Engineering, University of Fukui,*
3-9-1 Bunkyo, Fukui, Fukui, 910-8507, Japan

Abstract

This paper introduces our experience of applying the modified Ritchie-Knott-Rice (RKR) failure criterion (which predicts the occurrence of cleavage fracture when the mid-plane crack opening stress measured at four times the crack-tip opening displacement σ_{22d} exceeds a critical stress σ_{22c}) to the SE(B) specimen with a residual stress in the ductile to brittle transition temperature (DBTT) region. The fracture toughness test and elastic-plastic finite element analysis results are compared in this paper. 0.45 % carbon steel JIS S45C, whose tensile to yield stress ratio σ_B/σ_{YS} was equal to 1.5 at fracture test temperature was considered in this study. Focus was placed on whether the modified RKR failure criterion can be applied to the test specimen with a compressive residual stress that was introduced by a mechanical preload at room temperature. SE(B) specimen of width W x thickness B of 46 x 23 mm were chosen. Results showed that the scatter of σ_{22c}s obtained from specimens with a compressive residual stress were small difference. In addition, the J corresponding to the load that σ_{22d} first reaches σ_{22c} seemed to predict the lower bound toughness for the material and the specified specimen configuration.

Keywords — *Modified Ritchie-Knott-Rice failure criterion, Fracture toughness, SE(B) specimen, Compressive residual stress*

NOMENCLATURE

B	Specimen thickness
E	Young's modulus
J	J-integral
J_c	Fracture toughness
J_{cFEA}	J obtained at the fracture load P_c via EP-FEA
K_c	Stress intensity factor at fracture load P_c
K_{max}	Maximum SIF during precracking
K_{Jc}	$= [EJ_c/(1-\nu^2)]^{1/2}$: Fracture toughness expressed in terms of J
M	$= (W-a)\sigma_{YS}/J_c$: Parameter which gives information on the initial ligament size to fracture process zone size
P_c	Fracture load
P_{max}	Maximum force during precracking
P_{min}	Minimum force during precracking
V_g	Crack-mouth opening displacement (CMOD)
V_{LL}	Load line displacement
W	Specimen width
a	Crack length
x_j	Crack tip local coordinates (j = 1, 2, 3)
δ_t	Crack-tip opening displacement (CTOD)
ν	Poisson's ratio
ρ	Initial blunted notch
σ_{ij}	Stress components (i, j = 1, 2, 3)
σ_{YS0}	Nominal yield stress
σ_{B0}	Nominal tensile strength
σ_{YS}	True yield stress
σ_B	True tensile strength
σ_{22c}	Critical crack opening stress
σ_{22d}	Mid-plane crack-opening stress σ_{22} on the x_1 axis measured at a distance from the crack tip equal to four times the crack-tip opening displacement (CTOD) δ_t
σ_{22d0}	Converged value of σ_{22d}

ABBREVIATION

CTOD	Crack-Tip Opening Displacement
DBTT	Ductile-to-Brittle Transition Temperature
EP-FEA	Elastic-Plastic Finite Element Analysis
RKR	Ritchie-Knott-Rice
SE(B)	Single-Edge notched Bend bar

I. INTRODUCTION

Phenomenon of increasing the apparent fracture toughness of cracked body by subjecting a prior loading applied at higher temperature has been known as warm prestress (WPS) effect. The following three mechanisms as a cause of WPS effect are considered [1].

(1) Compressive residual stress ahead of the crack tip by preload
(2) Blunting of the crack tip
(3) Increase of deformation resistance due to work hardening ahead of the crack tip

Also, test specimen size effects on the cleavage fracture toughness J_c of a material in the ductile-to-brittle transition temperature (DBTT) region has been known to exist [2]-[5]. Large scatter in J_c has

also been known. Chen et al. have reported scatter of the fracture toughness, as follows; "it is necessary to distinguish the concepts of the minimum toughness or the lower boundary of toughness values from that of the scatter band of toughness. The former is a definite parameter determined by the specimen geometry and yielding properties and the latter is statistical behaviour determined by the distribution of the weakest constituent [6]". Meshii et al. interpreted Chen et al.'s opinion as that at least for the lower bound J_c can be reproduced by running an elastic-plastic finite element analysis (EP-FEA) with some failure criterion [7]-[9]. For this failure criterion, Meshii et al. considered the modified Ritchie-Knott-Rice (RKR) failure criterion, which predicts the occurrence of cleavage fracture when the crack-opening stress σ_{22}, measured at distance from the crack tip equal to four times the crack-tip opening displacement (CTOD) δ_t, hereinafter denoted as σ_{22d}, exceeds a critical value σ_{22c}. Though the J_c for specimens showed large variation for A533B [11] and S55C [10], the critical stress σ_{22c} showed small variation, approximately 5 and 4 % respectively. In the latter work, Meshii et al. suggested that the possibility of J when σ_{22d} first reaches σ_{22c} correspond to the lower bound J_c for specimen geometry [11].

This study is intended to examine the applicability of the modified RKR failure criterion to predict the occurrence of cleavage fracture of a SE(B) specimen with a compressive residual stress field induced by mechanical preload. The material considered was 0.45 % carbon steel JIS S45C. The fracture tests of the SE(B) specimen with compressive residual stress by preloading were conducted in the DBTT region. The specimen of width W x thickness B of 46 x 23 mm was chosen. By reproducing the test results by running large strain elastic-plastic finite element analysis (EP-FEA), it was demonstrated that the modified RKR failure criterion was applicable to the case with compressive residual stress.

II. MATERIAL SELECTION

The material considered was 0.45 % carbon steel JIS S45C, which was quenched at 850 °C and tempered at 550 °C. The chemical compositions of S45C were C: 0.47 %, Si: 0.17 %, Mn: 0.64 %, P: 0.009 %, S: 0.004 %, Cu: 0.02 %, Ni: 0.02 %, Cr: 0.02 %, respectively.

Charpy impact tests were conducted in accordance with JIS Z 2242. Charpy impact test results are shown in Fig. 1. From charpy impact test results, -10 °C and 23 °C were selected as the test temperature. Tensile tests were conducted in accordance with JIS Z 2241. As results, for the tensile test at 23 °C, nominal yield stress σ_{YS0} and nominal tensile strength σ_{B0} of 438 MPa and 718 MPa were obtained, respectively. For -10 °C, σ_{YS0} and σ_{B0} of 498 MPa and 760 MPa, respectively.

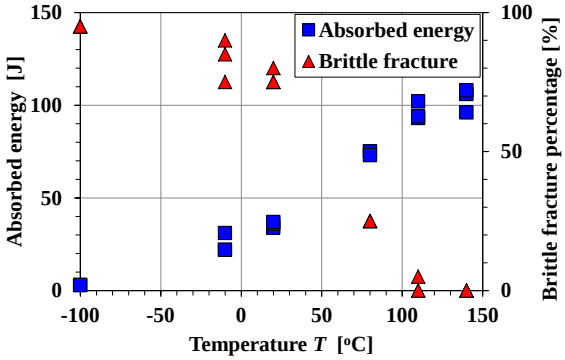

Fig. 1 Charpy Impact Test Results

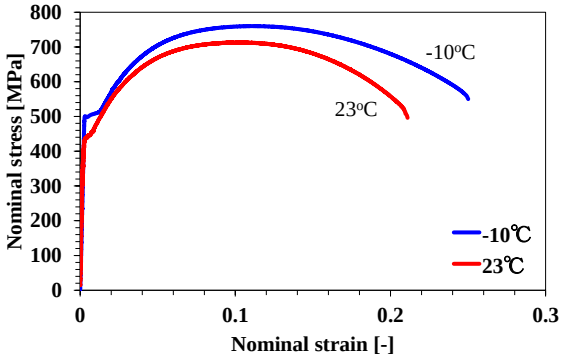

Fig. 2 Tensile Test Results

III.FRACTURE TOUGHNESS TESTS OF SE(B) SPECIMEN

Fracture toughness test for SE(B) specimen of width W x thickness B of 46 x 23 mm was conducted in accordance with ASTM E1921 [12]. The dimensions of SE(B) specimen are shown in Fig. 3.

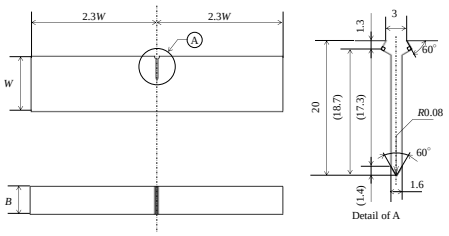

Fig. 3 Dimensions of SE(B) Specimen of 46 x 23 mm

TABLE 1 FRACTURE TOUGHNESS TEST RESULTS (S45C 46×23 MM SE(B), -10 °C)

Specimen id	6	7	9	10	11	μ	Σ	$2\Sigma/\mu$ [%]	(max-min)/min [%]
a/W	0.506	0.502	0.501	0.498	0.504	0.502	0.00	1.2	1.6
P_c [kN]	42.2	43.8	39.5	43.9	43.4	42.6	1.83	8.6	11.1
K_c [MPam$^{1/2}$]	93.1	95.1	85.7	94.3	94.9	92.6	3.95	8.5	11.0
J_c [N/mm]	52.1	70.0	41.9	52.6	67.3	56.8	11.7	41.2	67.1
K_{Jc} [MPam$^{1/2}$]	108.6	125.9	97.4	109.1	123.4	112.9	11.8	20.8	29.3
M	217	163	273	219	169	208	44.6	42.9	67.5

Length L and support span S of the specimen was requested to satisfy L/W = 4.5 and S/W = 4.0 and designed as L/W = 4.6 and S/W = 4.0, where width W = 46 mm. The residual stress was introduced to the crack-tip by mechanical pre-loading at room temperature before the fracture toughness test. Maximum preload was applied to 33 kN.

Precracking was performed with four discrete steps which satisfied the requirement of the standard that precracking can be performed by using at least two discrete steps. Fatigue precrack was inserted with loads corresponding to K_{max} = 19.8 and 13.8 MPam$^{1/2}$ for the 1st and last stages, respectively, which satisfied the requirement of the standard 25 and 15 MPam$^{1/2}$. For each discrete step, the reduction in P_{max} for any of these steps was 18 %, which satisfied the suggestion if the standard the reduction in P_{max} for any of these steps be no greater than 20 %. The maximum force P_{max} and the minimum force P_{min} ratio R = P_{min}/P_{max} = 0.1 was applied. The load frequency was 10 Hz.

In fracture toughness test, the loading rate was controlled to be the specified range of 0.1 to 2.0 MPam$^{1/2}$/s and resulted in the range of 1.18 to 1.22 MPam$^{1/2}$/s. Test temperature was requested to be held at -10 ± 3 °C for longer than 30B/25 minutes, where specimen thickness B is 23 mm, and result was -10 ± 1 °C for 45 minutes. The fracture test was conducted -10 °C, after precracking. 5 test results which satisfied the ASTM E1921 requirements were considered for examination.

Load vs. crack-mouth opening displacement (P-V_g) diagrams for the 5 tests are summarized in Fig. 4. Solid line in Fig. 4 shows V_g calculated from the elastic compliance given in ASTM E1820 [13]. The linear slope in the diagram showed good agreement with that calculated by the ASTM E1820 equation. As shown in Fig. 4, the path of the each P - V_g diagrams for 5 experiments showed reproducibility and thus the validity of the tests were confirmed. Fracture toughness J_c was obtained from the P - V_g diagram in accordance with ASTM E1921 and summarized in

table 1. In **table 1**, K_{Jc} is the fracture toughness in terms of stress intensity factor as following Eq.(1).

$$K_{Jc} = \sqrt{\frac{EJ_c}{1-\nu^2}} \quad (1)$$

Where Young's modulus E = 206 GPa and Poisson's ratio of ν = 0.3 was used in this conversion. The Standard deviation of a/W for each specimens were 0.00, and thus, possible J_c scatter due to crack depth difference was minimized. The averages of K_{Jc} were 112.9 MPam$^{1/2}$. The standard deviation of K_{Jc} was 11.8 MPam$^{1/2}$, and small compared with median value 24.6 MPam$^{1/2}$ that was predicted from equation (X4.1) in ASTM E1921. The 2 % tolerance bound K_{Jc} predicted from equation (X4.3) was 57.3 MPam$^{1/2}$, and thus, the obtained K_{Jc}s were sufficiently larger than this 2 % tolerance bound value. Minimum M was 163 and satisfied ASTM E1921's requirement M as following Eq. (2)

$$M = \frac{(W-a)\sigma_{YS}}{J_c} \geq 30 \quad (2)$$

Where W, a, and σ_{YS} are width, crack depth and yield stress of the specimen. From these observations, the test results were concluded as valid.

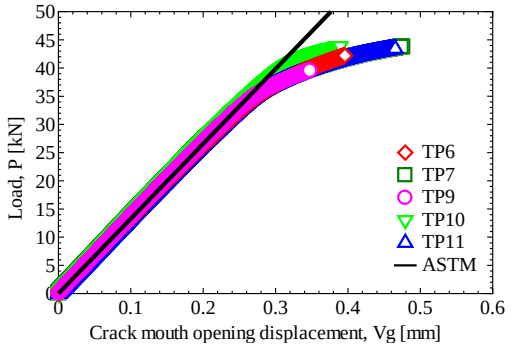

Fig. 4 *P*-*V*g Diagram (S45C 46 x 23 mm SE(B), -10 °C)

IV. FINITE ELEMENT ANALYSIS OF SE(B) SPECIMEN

Large-strain, EP-FEA were conducted for SE(B) specimen. FEA model used in this study is shown in Fig. 5. The width W was 46 mm and the

crack length a was 23 mm (a/W = 0.5). Considering symmetry conditions, one-quarter of the specimen was analysed. 20-node quadratic brick reduced integration element was used. An initial blunted notch of radius ρ was inserted at the crack tip. The CTOD was displacement at the intersection of a 90^o vertex with the crack franks. The J_c simulated by EP-FEA, denoted by J_{cFEA}, was evaluated using a load-vs.-crack mouth opening displacement (P-V_g) diagram, in accordance with ASTM E1820. The material behaviour in the EP- FEA was assumed isotropic hardening rule.

TABLE 2 4□T AND CRACK OPENING STRESS □22 AT THE FRACTURE LOAD P_C

Specimen ID	6	7	9	10	11	μ	Σ	$2\Sigma/\mu$ [%]	(max-min)/min (%)
J_{cFEA} [N/mm]	48.6	58.2	36.9	59.0	55.9	51.7	9.25	35.7	60.0
K_{JcFEA} [MPam$^{1/2}$]	104.9	114.8	91.4	115.6	112.5	107.8	10.1	18.8	26.5
$4\delta_t$ [mm]	0.120	0.151	0.084	0.154	0.144	0.131	0.03	45.0	84.1
σ_{22c} [MPa]	1831	1823	1851	1823	1824	1830	11.7	1.3	1.5

The Young's modulus E = 206 GPa and Poisson's ratio ν = 0.3 were used. The piecewise linear true stress-true strain curve of the S45C steel shown in Fig. 6 was used in the EP-FEA. The true stress-true strain data up to fracture was extrapolated by approximating the tensile test results with the Ramberg-Osgood equation shown in Eq. (3). The parameters of Eq. (1) are shown in table 3. Abaqus [14] was used as a FEA solver.

$$\frac{\varepsilon}{\varepsilon_0}=\frac{\sigma}{\sigma_0}+\alpha\left(\frac{\sigma}{\sigma_0}\right)^n \quad (3)$$

Where if $\sigma < \sigma_0$, $\varepsilon = \sigma/E$, σ, ε are true stress and true strain, σ_0 is reference stress (= σ_{YS} in this study), α, n are material constant. To avoid local large deformations at loaded and supported nodes, the elements surrounding these nodes were set to be linearly elastic.

Constraints were also imposed for the nodes along the line of support. Load line displacement was applied and load was measured as the total reaction force of the supporting nodes. To accurately reproduce the tests, first, load was increased to 33 kN with material parameters of room temperature, and then reloaded. After a compressive residual stress was introduced to the crack tip, material parameters were changed with those of -10 °C. Finally, load was increased to simulate the maximum load observed in experiments.

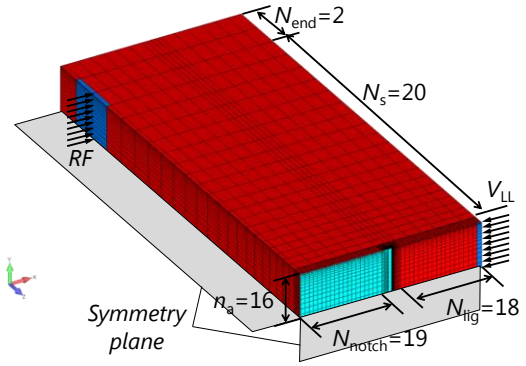

Fig. 5 Finite Element Model of SE(B) Specimen

TABLE 3 SUMMARY OF PARAMETER FOR RAMBERG-OSGOOD PLASTICITY MODEL

Temperature [°C]	σ_0 [MPa]	α	n
-10	499	3.00	4.81
RT	439	2.75	4.52

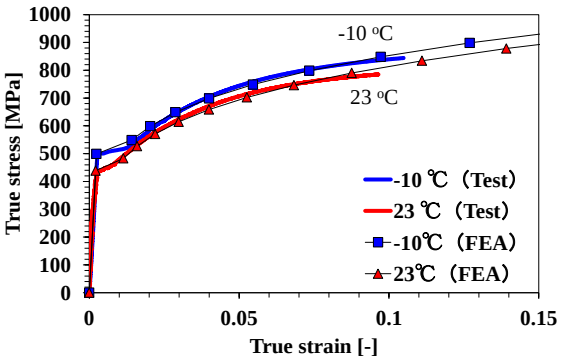

Fig. 6 True stress-true strain curve for EP-FEA

V. RESULTS OF EP-FEA

P-V_g diagrams obtained from the EP-FEA are shown in **Fig. 7**. The FEA result in **Fig. 7** was close to the experimental results.

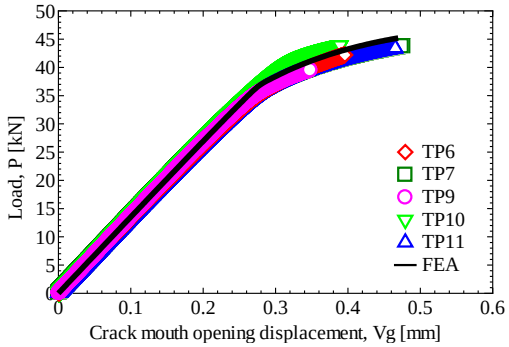

Fig. 7 Comparison of FEA and experimental P-V_g diagrams

FEA fracture toughness J_c, denoted as J_{cFEA}, was obtained from the P-V_g diagram in accordance with ASTM E1921 and summarized in table 2. The critical value σ_{22c} of the modified RKR failure criterion was also summarized in table 2. From table 2, it is read that though J_{cFEA} ranged in 36.9 to 59.0 N/mm and showed large variation of 60.0 %, σ_{22c}s at the fracture load P_cs ranged in 1823 to 1851, and thus only 1.5 % variation. On this point, it was concluded that the modified RKR failure criterion is applicable to S45C SE(B) specimens with compressive residual stress.

VI. DISCUSSION

The relationship between σ_{22} measured at $4\delta_t$ on the x_1 axis, denoted as σ_{22d}, and J_{FEA} calculated from P-V_g diagram for each load step are shown in Fig. 8. The solid line in Fig. 8 is the average of σ_{22c}. From Fig. 8, saturating nature of σ_{22d} for increasing

J_{FEA} is read. The small scatter of σ_{22c} seemed to be a result that σ_{22c} is a saturated value of σ_{22d}. Meshii et al. reported that J when σ_{22d} reaches σ_{22c} has the possibility to correspond to the lower bound of J_c for specified specimen geometry [11]. Thus, it was examined whether their finding is applicable to the case considered with compressive residual stress. Although σ_{22d} in Fig. 8 showed a tendency of convergence with increasing J_{FEA}, there is not a definite way to determine whether σ_{22d} has converged or not numerically. Hence, we applied a method described below. First, relationship between σ_{22d} and J_{FEA} is fitted by Eq. (4).

$$\frac{\sigma_{22d}}{\sigma_{YS}} = \alpha_1 \tanh(\beta_1 J_{FEA}) + \alpha_2 \frac{2}{\pi} \tan^{-1}(\beta_2 J_{FEA}) + \left(\frac{\sigma_{22d}}{\sigma_{YS}}\right)_{J_{FEA}=0} \quad (4)$$

$$\lim_{J_{FEA}\to\infty} \frac{\sigma_{22d}}{\sigma_{YS}} = \alpha_1 + \alpha_2 + \left(\frac{\sigma_{22d}}{\sigma_{YS}}\right)_{J_{FEA}=0} \quad (5)$$

$$th = \left(\frac{\sigma_{22d}}{\sigma_{YS}}\right) \Bigg/ \left[\alpha_1 + \alpha_2 + \left(\frac{\sigma_{22d}}{\sigma_{YS}}\right)_{J_{FEA}=0}\right] \quad (6)$$

Then J at the value of th defined as Eq. (6) is equal to 0.95 was defined as the predicted lower bound of J_c, denoted as J_s. In this work, J_s was 18.6 N/mm, and thus, the predicted lower bound K_{Js} was 64.9 MPam$^{1/2}$ when σ_{22d0} = 1844 MPa. On the other hand, 2 % tolerance bound $K_{Jc(0.02)}$ of the experimental data by the method of ASTM E1921 is 57.3 MPam$^{1/2}$, and thus, K_{Js} was closed. In summary, although it is necessary to study further for more appropriate method of determining the convergence value of the σ_{22d} and threshold to J at the value of Eq. (6), it seems that J_s was able to predict the lower bound of J_c in an engineering sense, even for a case with compressive residual stress.

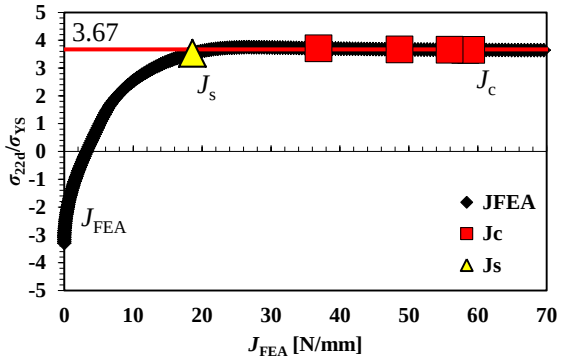

Fig. 8 The relationship between σ_{22d} and J_{FEA} calculated from P-V_g diagram

VII. CONCLUSION

In this work, applicability of the modified RKR failure criterion was demonstrated for S45C SE(B) specimen with compressive residual stress due to preloading.

ACKNOWLEDGMENT

Experiment of this paper is supported by Mr. Naohiro Kikuya, Graduate School of Engineering, University of Fukui. The authors would like to thank for his support.

REFERENCES

[1] F. M. Beremin, "Numerical modelling of warm prestress effect using damage function for cleavage fracture," Proc. Conf. ICF 5, 5, pp 825-832, 1981.

[2] K. Wallin, "The Size Effect in K_{IC} Results," Engineering Fracture Mechanics, 22, pp. 149-163, 1985.

[3] R. H. Dodds, T. L. Anderson, and M. T. Kirk, "A Framework to Correlate a/W Ratio Effects on Elastic-Plastic Fracture Toughness (J_c)," International Journal of Fracture, 48, pp. 1-22, 1991.

[4] M. Nevalainen, R. H. Dodds, "Numerical Investigation of 3-D Constraint Effects on Brittle Fracture in SE(B) and C(T) Specimens," International Journal of Fracture, 74, pp. 131-161, 1995.

[5] H. J. Rathbun, G. R. Odette, T. Yamamoto, M. Y. He, and G. E. Lucas, "Statistical and Constraint Loss Size Effects on Cleavage Fracture–Implications to Measuring Toughness in the Transition," Journal of Pressure Vessel Technology, 128, pp. 305-313, 2005.

[6] J. H. Chen, G. Z. Wang, C. Yan, H. Ma, and L. Zhu, "Advances in the Mechanism of Cleavage Fracture of Low Alloy Steel at Low Temperature," Part II: Fracture model, International Journal of Fracture, 83, pp. 121-138, 1997.

[7] K. Lu, T. Meshii, "Application of T_{33}-Stress to Predict the Lower Bound Fracture Toughness for Increasing the Test Specimen Thickness in the Transition Temperature Region," Advances in Materials Science and Engineering, pp. 1-8, 2014.

[8] T. Meshii, K. Lu, and Y. Fujiwara, "Extended Investigation of the Test Specimen Thickness (TST) Effect on the Fracture Toughness (J_c) of a Material in the Ductile-to-Brittle Transition Temperature Region as a Difference in the Crack Tip Constraint − What Is the Loss of Constraint in the TST Effects on J_c?," Engineering Fracture Mechanics, 135, pp. 286-294, 2015.

[9] T. Meshii, T. Yamaguchi, and Y. Higashino, "Applicability of the Modified Ritchie-Knott-Rice Failure Criterion to Examine the Feasibility of Miniaturized Charpy Type SE(B) Specimens," Advances in Materials Science and Engineering, (submitted), 2016.

[10] T. Meshii, K. Lu, and R. Takamura, "A Failure Criterion to Explain the Test Specimen Thickness Effect on Fracture Toughness in the Transition Temperature Region," Engineering Fracture Mechanics, 104, pp. 184-197, 2013.

[11] T. Meshii, T. Yamaguchi, "Applicability of the Modified Ritchie-Knott-Rice Failure Criterion to Transfer of Fracture Toughness J_c of Reactor Pressure Vessel Steel Using Specimens of Different Thicknesses-Possibility of Deterministic Approach to Transfer the Minimum J_c for Specified Specimen Thicknesses," Theoretical and Applied Fracture Mechanics, (in press, http://dx.doi.org/10.1016/j.tafmec.2016.04.002), 2016.

[12] ASTM, "E1921-10 Standard Test Method for Determination of Reference Temperature, T_o, for Ferritic Steels in the Transition Range," Annual Book of ASTM Standards, American Society for Testing and Materials, Philadelphia PA., 2010.

[13] ASTM, "E1820-06a Standard Test Method for Measurement of Fracture Toughness," Annual Book of ASTM Standards, American Society for Testing and Materials, Philadelphia PA., 2006.

[14] Abaqus version 6.14, "Abaqus Analysis User's Manual," Dassault Systemes Simulia Corp., USA., 2014